

Proceeding Paper

# 1,4-Butane-Sultone Functionalized Graphitic Carbon Nitride as a Highly Efficient Heterogeneous Catalyst for the Synthesis of Quinazolines Derivatives <sup>†</sup>

Hossein Ghafuri <sup>\*</sup>, Zahra Nasri and Zeinab Tajik

Catalysts and Organic Synthesis Research Laboratory, Department of Chemistry, Iran University of Science and Technology, Tehran 16846-13114, Iran; e-mail@e-mail.com (Z.N.); e-mail@e-mail.com (Z.T.)

<sup>\*</sup> ghafuri@iust.ac.ir.

<sup>†</sup> Presented at the 26th International Electronic Conference on Synthetic Organic Chemistry; Available online: <https://ecsoc-26.sciforum.net..>

**Abstract:** 1,4-Butane-sultone functionalized graphitic carbon nitride nanosheets (g-C<sub>3</sub>N<sub>4</sub>@Bu-SO<sub>3</sub>H) was prepared and applied as an efficient heterogeneous catalyst for the synthesis of various quinazolines derivatives with high yield. In next step, the structure and morphology of catalyst was characterized by different analyses such as, FT-IR, EDS, XRD and FE-SEM. On the other side, considering the noticeable features of g-C<sub>3</sub>N<sub>4</sub>@Bu-SO<sub>3</sub>H such as high stability, easy to synthesize, non-toxicity, excellent reusability, and so on, the synthesis of quinazolines with numerous advantages such as short reaction time, mild reaction condition, easy separation and etc were realized.

**Keywords:** 1,4-Butane-sultone; graphitic carbon nitride; quinazolines derivatives; heterogeneous catalyst

**Citation:** Ghafuri, H.; Nasri, Z.; Tajik, Z. 1,4-Butane-Sultone Functionalized Graphitic Carbon Nitride as a Highly Efficient Heterogeneous Catalyst for the Synthesis of Quinazolines Derivatives. *Chem. Proc.* **2022**, *4*, x. <https://doi.org/10.3390/xxxxx>

Academic Editor: Julio A. Seijas

Published: 15 November 2022

**Publisher's Note:** MDPI stays neutral with regard to jurisdictional claims in published maps and institutional affiliations.



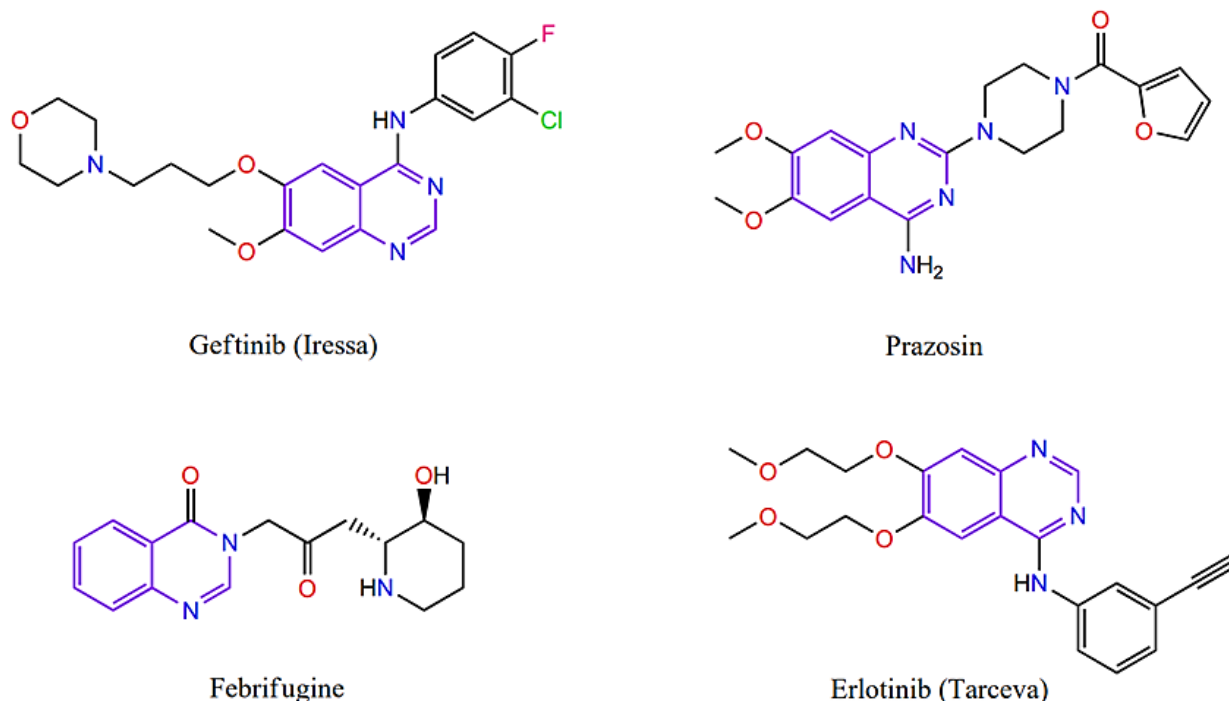
**Copyright:** © 2022 by the authors. Submitted for possible open access publication under the terms and conditions of the Creative Commons Attribution (CC BY) license (<https://creativecommons.org/licenses/by/4.0/>).

## 1. Introduction

Quinazolines and their derivatives are as a significant class of nitrogen-containing heterocyclic scaffolds that the structure of these compounds have been formed from six-membered fused rings [1]. Accordingly, these quinazolines derivatives have numerous biological activities, including anticancer, antimalaria, antimicrobial, antiviral, anti-HIV, anti-inflammatory, antifungal, acaricidal, weedicide, antidepressant, anticonvulsant, muscle relaxant, and so on [2,3]. On the other side, because of various biological values, they are utilized for synthesis of considerable drugs such as prazosin (treatment of benign prostatic obstruction) [4], gefitinib (antitumor therapeutic agents) [5,6], erlotinib (EGFR inhibitor) [7], lapatinib (tyrosine kinase inhibitor) [8], alfuzosin (anticancer) [9], febrifugine (antimalaria) [10], and etc (Scheme 1).

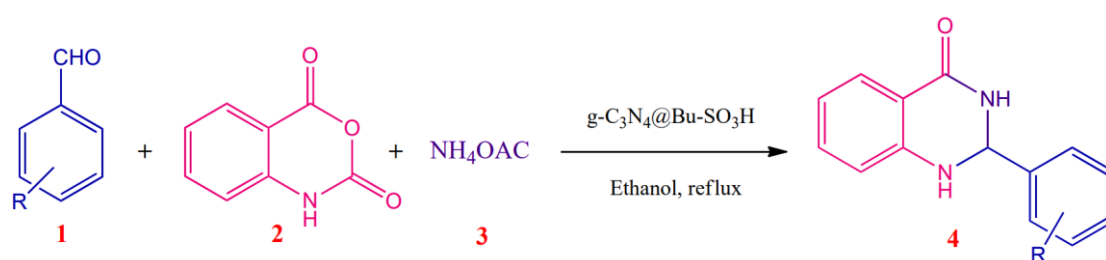
Recently, the preparation of quinazolines derivatives has been heeded as the basic structure of the most bioactive medicines [11]. Therefore, to apply an effective and excellent catalyst is a noticeable approach to develop the synthesis of them with high yield. Because of various advantages such as, photocatalytic activity, wastewater treatment, organic transformation, disinfection, healthcare, environmental, electrochemical biosensor, CO<sub>2</sub> reduction, and H<sub>2</sub> generation [12,13]. Graphitic carbon nitride (g-C<sub>3</sub>N<sub>4</sub>) is considered as catalytic support for synthesis of different heterogeneous catalyst. In addition, Among the various catalytic methods, the use of metal-free heterogeneous catalysts is one of the best methods due to its green nature, easy synthesis and separation [14]. Although, there are different types of metal and metal-free catalysts such as PBDS-SCMNPs ionic liquid [15], Wang-OSO<sub>3</sub>H [16], Silica sulfuric acid [17], titanium silicon oxide [18], montmorillonite-KSF [19], SrCl<sub>2</sub>·6H<sub>2</sub>O [20], and Y(NO<sub>3</sub>)<sub>3</sub>·6H<sub>2</sub>O [21] that have been used for the synthe-

sis of these heterocyclic derivatives but These catalysts have disadvantages and limitations such as difficult and long synthesis steps, expensive reagents, high reaction temperature, and low stability that lead to importance of the synthesis and characterization of suitable metal-free catalyst that can be beneficial for eliminating these disadvantages.



**Scheme 1.** Some of the pharmaceutical active compounds containing quinazoline structures.

In this work, a high efficient metal-free heterogeneous catalyst ( $g\text{-C}_3\text{N}_4@Bu\text{-SO}_3\text{H}$ ) was prepared and applied for synthesis of 2,3-dihydroquinazoline and its derivatives with excellent advantages consisting of short reaction time, inexpensive and available raw materials, no oxidant, and high selectivity (Scheme 2).



**Scheme 2.** Multi-component reaction for synthesis of dihydroquinazolines derivatives.

**Table 1.** Synthesis of 2,3-dihydroquinazoline derivatives using  $g\text{-C}_3\text{N}_4@Bu\text{-SO}_3\text{H}$  metal-free catalyst.

Entry	R	Product	Time (min)	Mp (°C)	Yield
1	H	4a	15	207–210	90
2	4-Cl	4b	15	203–206	96
3	2-Cl	4c	15	205–206	95
4	4-NO <sub>2</sub>	4d	20	201–202	90
5	3-OH	4e	30	212–216	89

Reaction conditions: benzaldehyde (1 mmol), isotonic anhydride (1 mmol), and ammonium acetate (1 mmol).  $g\text{-C}_3\text{N}_4@Bu\text{-SO}_3\text{H}$  (20 mg) and ethanol (7 mL) under reflux conditions.

## 2. Experimental

### 2.1. Material

All chemicals were purchased from Sigma-Aldrich Co and Merck. Fourier Transform Infrared (FTIR) spectra were recorded on Tensor27. Nuclear Magnetic Resonance (NMR) data were acquired on a Varian-Inova 500MHz. X-Ray Diffraction (XRD) patterns were obtained using Dron-8 diffractometer. Energy-dispersive X-ray (EDX) spectrum was recorded on Numerix DXP-X10P. Field Emission Scanning Electron Microscopy (FESEM) images were recorder with TESCAN-MIRA III.

### 2.2. Preparation of Bulk $g\text{-C}_3\text{N}_4$ and Nanosheets

First, the melamine powder was heated at 550 °C in furnace in air atmosphere at the heating rate 2.5 °C/min for 4 h. Then, the obtained yellow powder was well ground with a mortar to obtain a blended solid powder. In next step, for the synthesis of  $g\text{-C}_3\text{N}_4$  nanosheets, bulk  $g\text{-C}_3\text{N}_4$  (1.0 g) was stirred with  $\text{H}_2\text{SO}_4$  (20.0 mL) at 90 °C for 5 h. The resulting mixture was stirred by (200 mL) ethanol in room temperature at 2 h and it remained constant until all the material was settled. After 2 days, the resulting mixture was dispersed by ultrasonic probe at 300 W for 1.5 h. Eventually, the formed suspension was washed three times by ethanol and seven times by distilled water. After that, white product was dried in oven at 60 °C.

### 2.3. Preparation of Graphitic Carbon Nitride Nanosheets Functionalized with 1,4-Butane-sultone ( $g\text{-C}_3\text{N}_4\text{@Bu-SO}_3\text{H}$ )

First, the  $g\text{-C}_3\text{N}_4$  nanosheets (1.0 g) were dispersed in toluene (25 mL), after that 1,4-butane-sultone (3.0 g) was added the reaction mixture and was refluxed under nitrogen atmosphere for 6 h. Finally, the resulting product got cold in room temperature, then it was centrifuged and washed with chloroform and ethyl ether solvents, and dried in oven at 60 °C.

### 2.4. Selected Spectral Data

#### 2-Phenyl-2, 3-dihydro-4(1H)-quinazolinone (4a)

FTIR (KBr,  $\text{cm}^{-1}$ ): 3300, 3176, 2981, 1651, 1610, 1507, 1440, 1385, 745  $\text{cm}^{-1}$ .  $^1\text{H}$  NMR (500 MHz, DMSO):  $\delta$  H (ppm) = 5.75(s, 1H, CH), 6.67(t, 1H, Ar-H), 6.74(d, 1H, Ar-H), 7.1(s, 1H, NH), 7.23(t, 1H, Ar-H), 7.34(t, 1H, Ar-H), 7.38(t, 1H, Ar-H), 7.49(d, 1H, Ar-H), 7.60(d, 1H, Ar-H), 8.27(s, 1H, CONH).

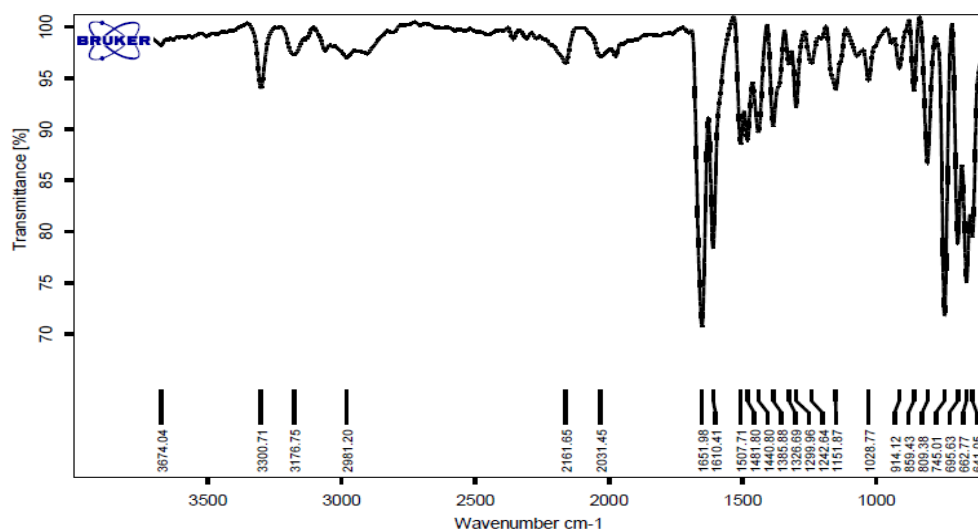


Figure 1. FT-IR spectrum of the 2-phenyl-2, 3-dihydro-4(1H)-quinazolinone.

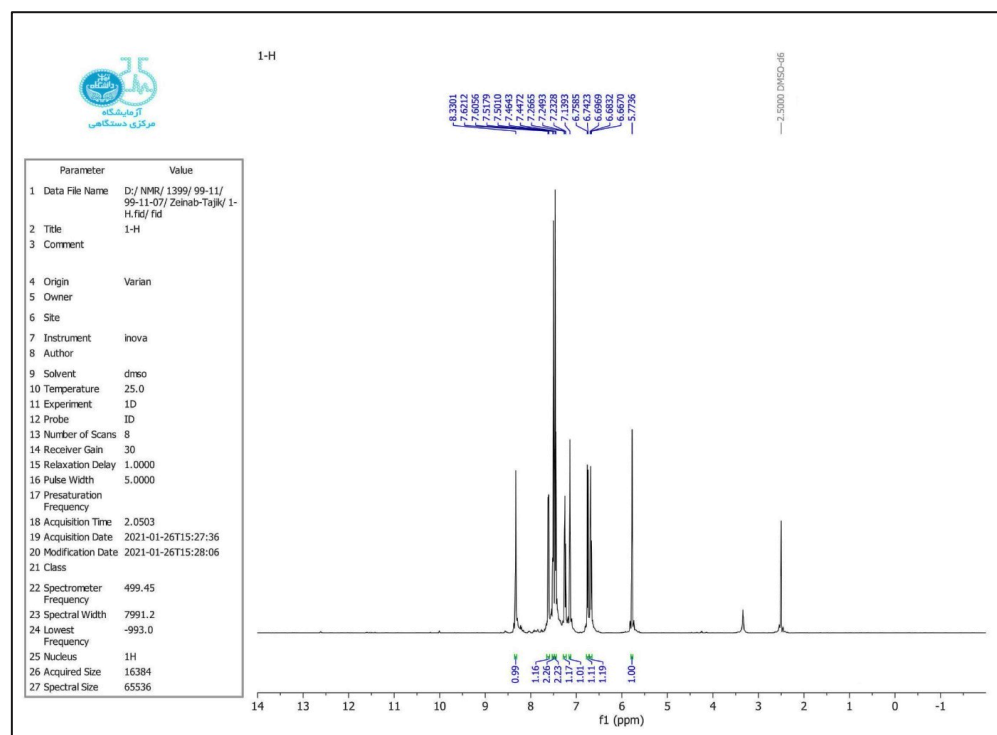


Figure 2.  $^1\text{H}$ NMR spectrum of the 2-phenyl-2, 3-dihydro-4(1H)-quinazolinone.

#### 2-(4-Chloro-phenyl)-2, 3-dihydro-1H-quinazoline-4-one (4b)

FTIR (KBr,  $\text{cm}^{-1}$ ): 3305, 3184, 3062, 1654, 1606, 1431, 1090, 749  $\text{cm}^{-1}$ .  $^1\text{H}$  NMR (500 MHz, DMSO):  $\delta$  H (ppm) = 5.77(s, 1H, CH), 6.68(t, 1H, Ar-H), 6.74(d, 1H, Ar-H), 7.1(s, 1H, NH), 7.24(t, 1H, Ar-H), 7.45(d, 1H, Ar-H), 7.50(d, 1H, Ar-H), 7.61(d, 1H, Ar-H), 8.27(s, 1H, CONH).

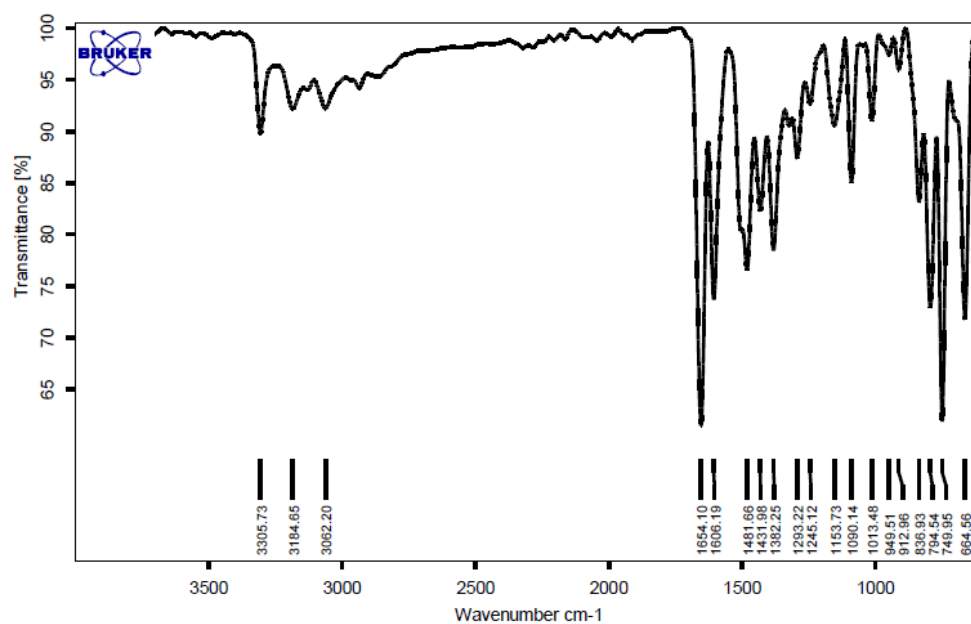
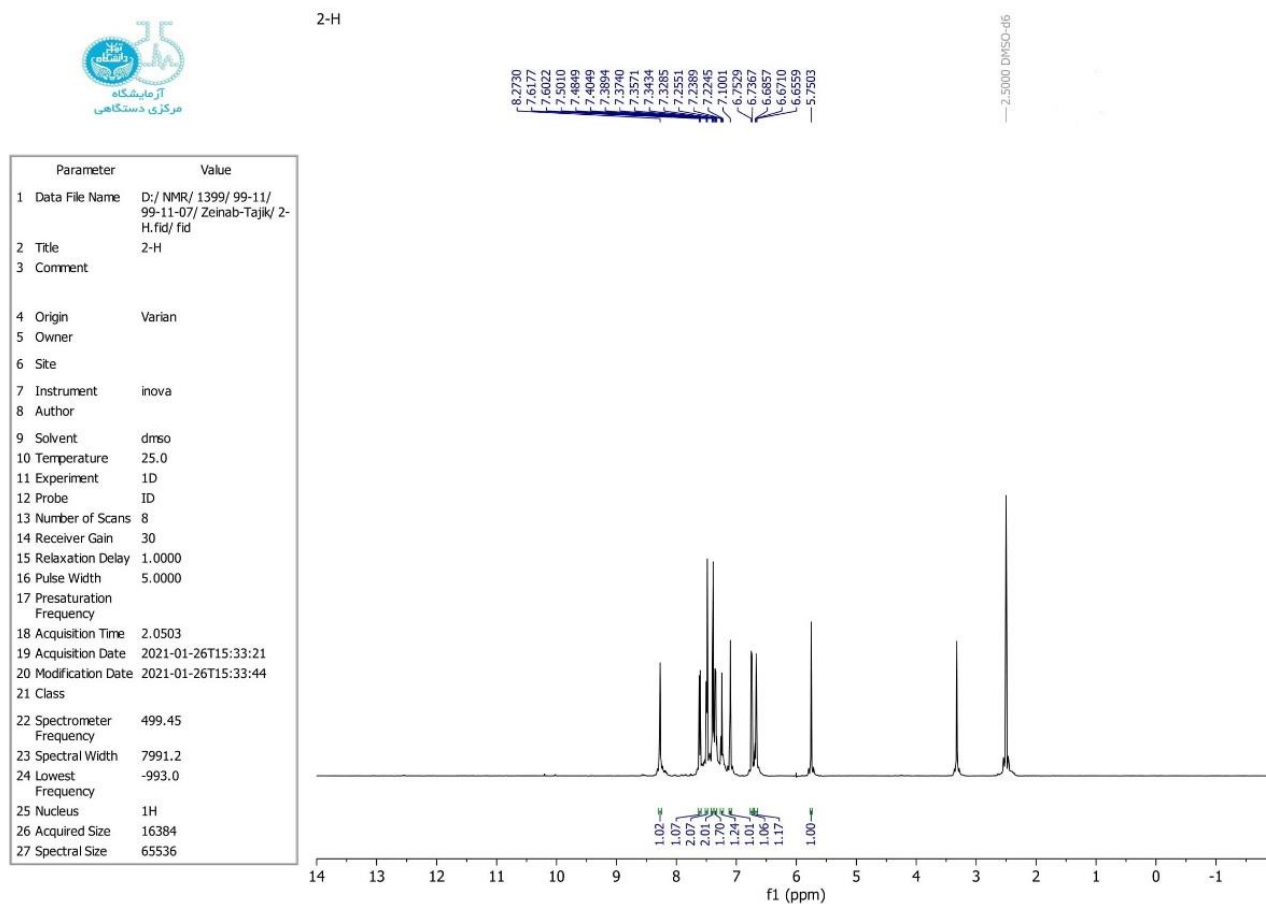


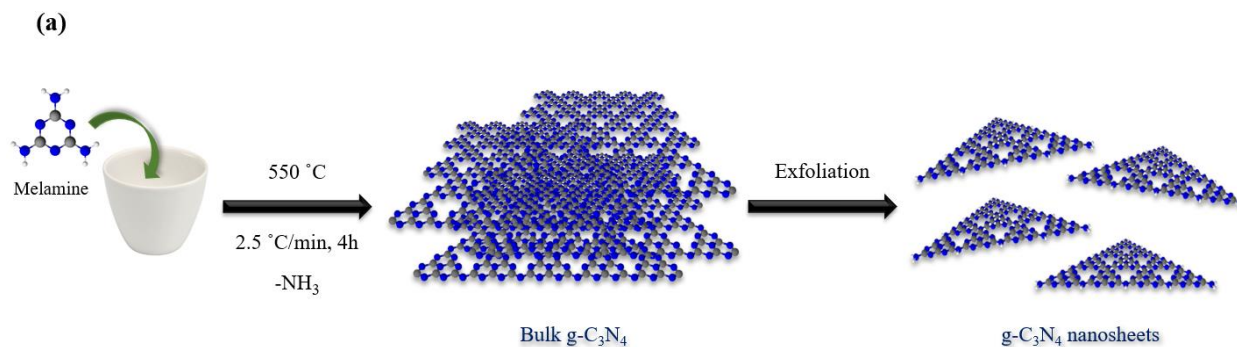
Figure 3. FT-IR spectrum of the 2-(4-chloro-phenyl)-2, 3-dihydro-1H-quinazoline-4-one.

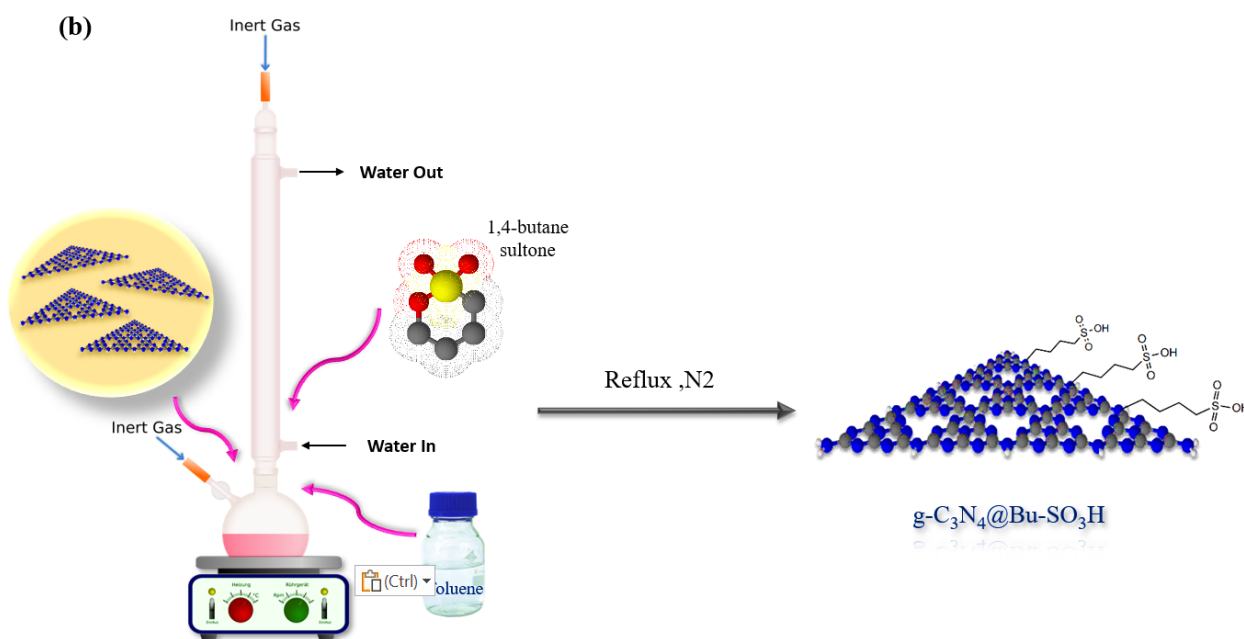


**Figure 4.**  $^1\text{H}$ NMR spectrum of the 2-(4-chloro-phenyl)-2,3-dihydro-1H-quinazolin-4-one.

### 3. Results and Discussion

The  $\text{g-C}_3\text{N}_4@ \text{Bu-SO}_3\text{H}$  heterogeneous catalyst was synthesized in just three steps (Scheme 3). In the first step, bulk  $\text{g-C}_3\text{N}_4$  was prepared by polymerization of melamine. In the second step, the morphology of bulk  $\text{g-C}_3\text{N}_4$  was changed to  $\text{g-C}_3\text{N}_4$  nanoparticle. Finally,  $\text{g-C}_3\text{N}_4$  nanoparticle was functionalized with 1,4-butane-sultone. This catalyst was proved by different analyses such as Fourier Transform Infrared (FT-IR) Spectroscopy, Energy Dispersive Spectrometer (EDS), Field Emission Scanning Electron Microscopy (FE-SEM), and X-ray diffraction analysis (XRD) [22].

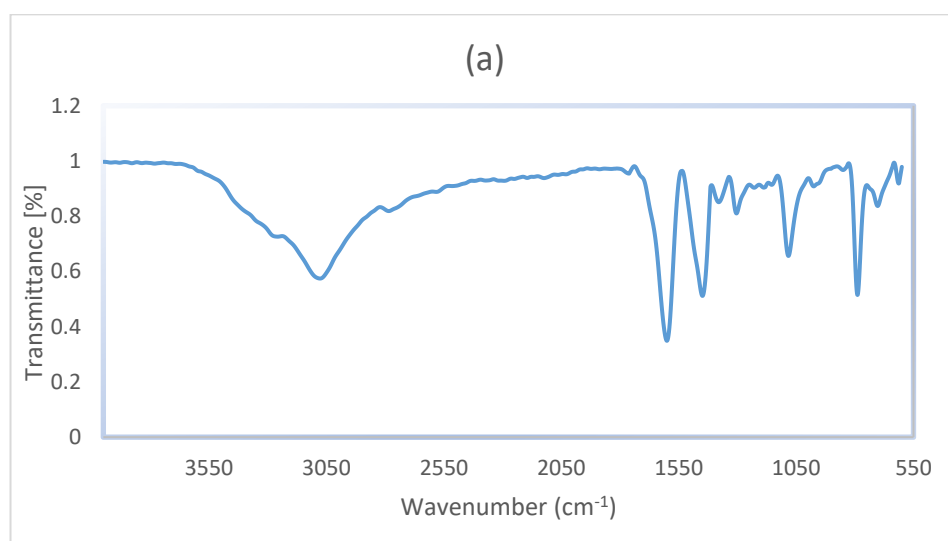


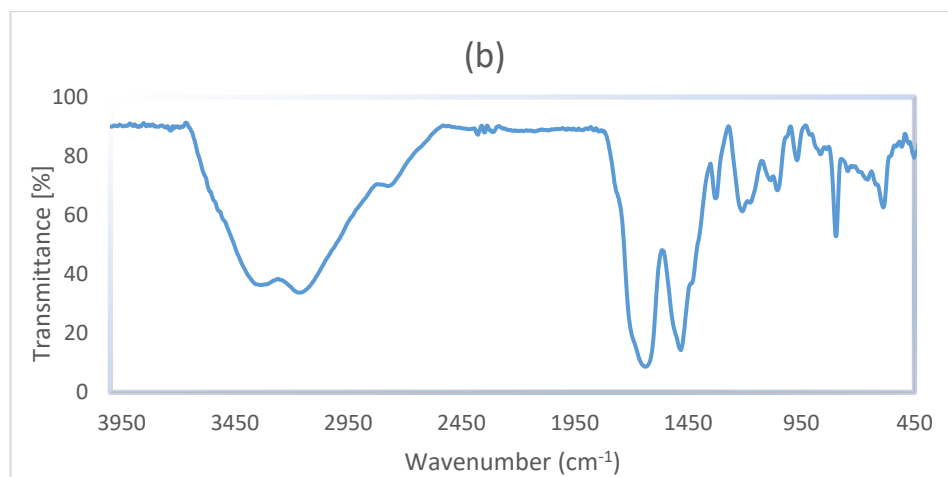


**Scheme 3.** Synthesis of  $g-C_3N_4$  nanosheets (a),  $g-C_3N_4@Bu-SO_3H$  (b).

The FT-IR spectra of  $g-C_3N_4$  nanoparticle (a) and  $g-C_3N_4@Bu-SO_3H$  (b) have been showed in Figure 5. A relatively strong peak in the range of  $3000$  to  $3300\text{ cm}^{-1}$  is related to stretching vibration of N–H bonds, the  $1602\text{ cm}^{-1}$  peak is related to C=N stretching vibration modes. The absorption peak of C–N bonds observed in rang of  $1303$  and  $1082\text{ cm}^{-1}$  that can be attributed to C–N bonds between triazine and N–H groups. On the other hand, the characteristic peaks at  $1448$  and  $1379\text{ cm}^{-1}$  are related to C–N ring bonds and finally, the peak at  $784\text{ cm}^{-1}$  may be related to tri-s-triazine units (Figure 5a).

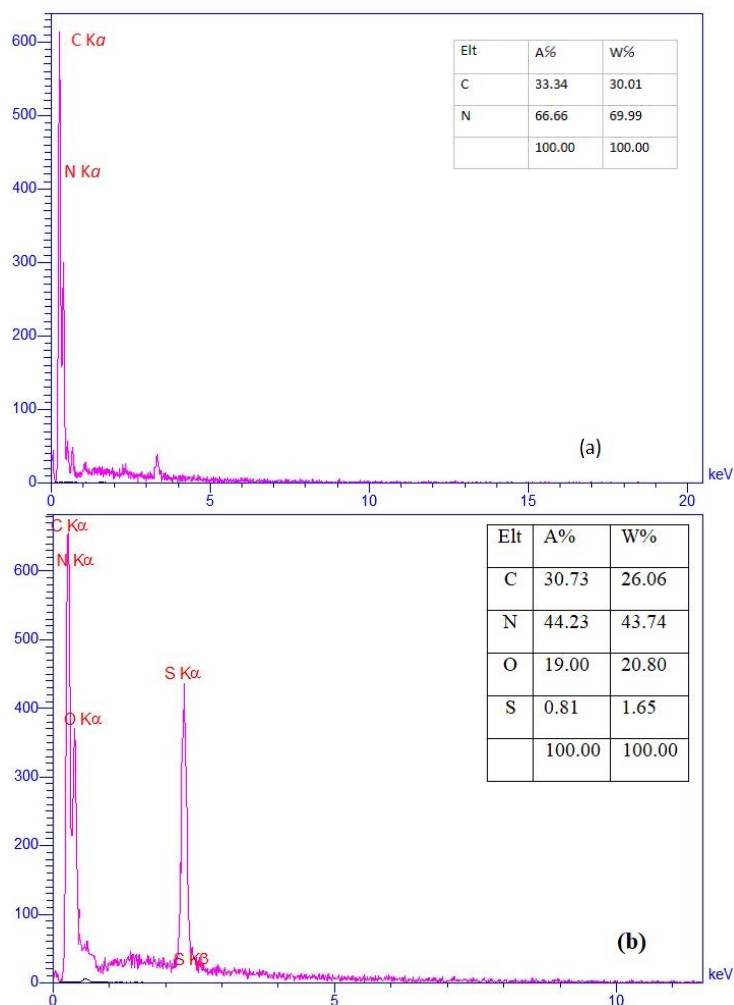
In The spectrum of  $g-C_3N_4@Bu-SO_3H$ , which is shown in Figure 5b, the two peaks  $2781$  and  $2758\text{ cm}^{-1}$  are related to C–H groups in 1,4-butane-sultone. The symmetric and asymmetric stretching vibration modes of  $SO_2$  have appeared in the regions  $1220$  and  $1348\text{ cm}^{-1}$ , the characteristic peaks at  $1176$  and  $1207\text{ cm}^{-1}$  are related to S–OH bonds.





**Figure 5.** The FT-IR spectra of g-C<sub>3</sub>N<sub>4</sub> nanosheets (a), g-C<sub>3</sub>N<sub>4</sub>@Bu-SO<sub>3</sub>H catalyst (b).

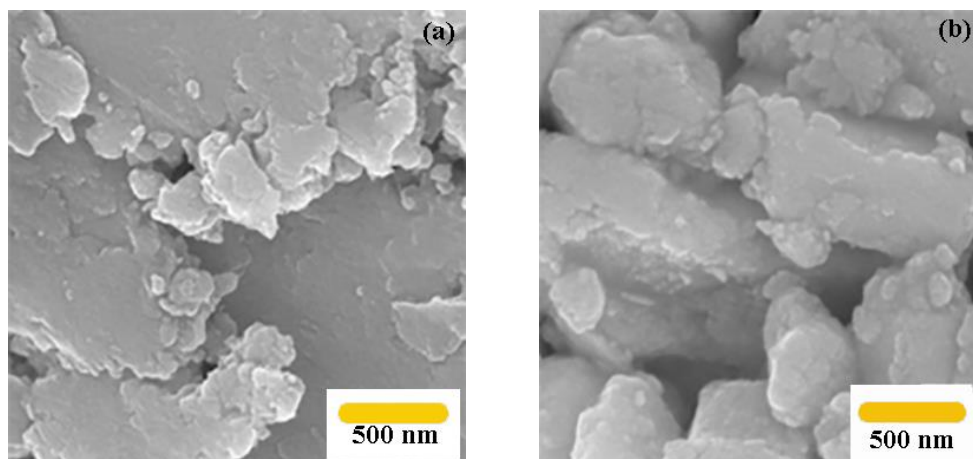
In the Figure 6a, the presence of carbon and nitrogen atoms in structure of g-C<sub>3</sub>N<sub>4</sub> nanoparticle was confirmed by the EDS analysis. As shown in the Figure 6b, the presence of oxygen and sulfur elements proves synthesis of desired catalyst (g-C<sub>3</sub>N<sub>4</sub>-Bu-SO<sub>3</sub>H).



**Figure 6.** EDS spectra of g-C<sub>3</sub>N<sub>4</sub> nanosheets (a), g-C<sub>3</sub>N<sub>4</sub>@Bu-SO<sub>3</sub>H (b).

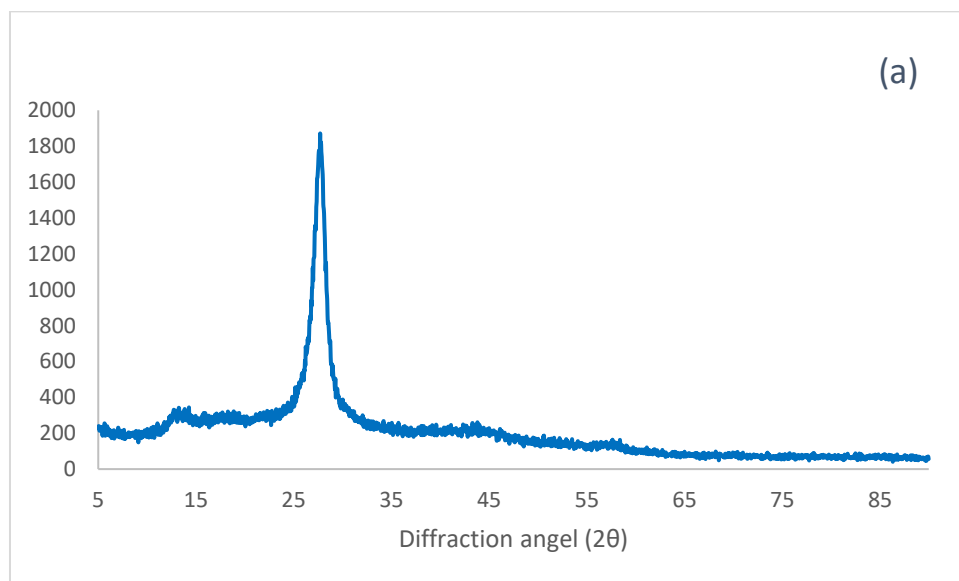
The morphology of g-C<sub>3</sub>N<sub>4</sub> nanosheets and g-C<sub>3</sub>N<sub>4</sub>@Bu-SO<sub>3</sub>H were shown by The FE-SEM images. In the Figure 7a, the g-C<sub>3</sub>N<sub>4</sub> nanosheets have a relatively flat surface, while

in the Figure 7b, image of  $g\text{-C}_3\text{N}_4\text{@Bu-SO}_3\text{H}$  is partly different and irregular. Therefore, this variance can verified the deposition of sultone on the  $g\text{-C}_3\text{N}_4$  nanosheets.



**Figure 7.** FE-SEM image of  $g\text{-C}_3\text{N}_4$  nanosheets (a),  $g\text{-C}_3\text{N}_4\text{@Bu-SO}_3\text{H}$  (b).

The XRD pattern of  $g\text{-C}_3\text{N}_4$  nanoparticle and  $g\text{-C}_3\text{N}_4\text{@Bu-SO}_3\text{H}$  can be seen in Figure 8. Diffraction peaks at  $2\theta$ :  $27.35^\circ$  (002) and  $13.04^\circ$  (100) are related  $g\text{-C}_3\text{N}_4$  nanoparticle (Figure 8a). Also diffraction peaks at  $2\theta$ :  $27.4^\circ$  (002),  $2\theta = 17.9^\circ$ , and  $14.8^\circ$  (100) are related to the  $g\text{-C}_3\text{N}_4\text{@Bu-SO}_3\text{H}$  that approve synthesis of this catalyst (Figure 8b).





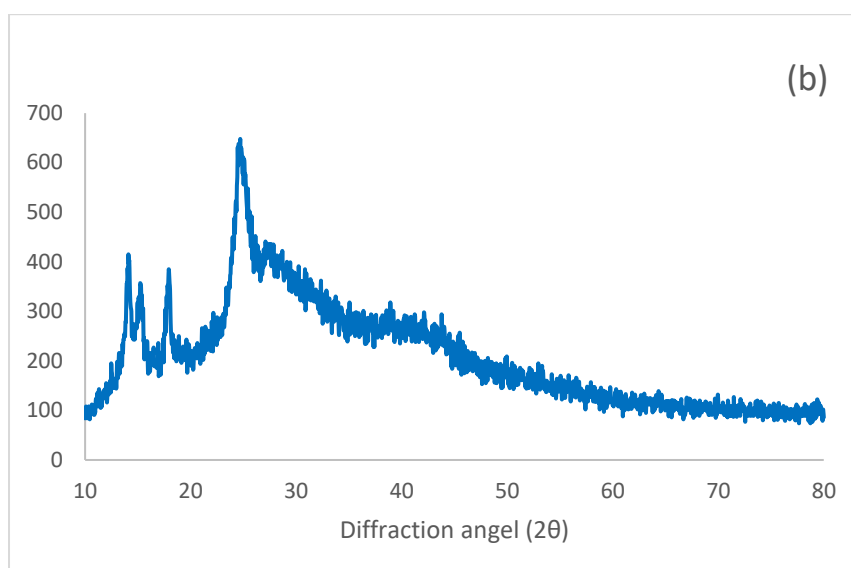


Figure 8. XRD spectra of g-C<sub>3</sub>N<sub>4</sub> nanosheets (a), g-C<sub>3</sub>N<sub>4</sub>@Bu-SO<sub>3</sub>H (b).

#### 4. Conclusions

In summary, an efficient heterogeneous catalyst (g-C<sub>3</sub>N<sub>4</sub>@Bu-SO<sub>3</sub>H) was synthesized and utilized for production of quinazolines derivatives with highly advantages such as short reaction time, mild condition, and easy separation. On the other side, this catalyst can be used and recycled for five times with high yield.

#### References

- Chen, J.; Chang, D.; Xiao, F.; Deng, G.J. Four-component quinazoline synthesis from simple anilines, aromatic aldehydes and ammonium iodide under metal-free conditions. *Green Chem.* **2018**, *20*, 5459–5463.
- Asif, M. Chemical characteristics, synthetic methods, and biological potential of quinazoline and quinazolinone derivatives. *Int. J. Med. Chem.* **2014**, *2014*.
- Gupta, T.; Rohilla, A.; Pathak, A.; Akhtar, M.J.; Haider, M.R.; Yar, M.S. Current perspectives on quinazolines with potent biological activities: A review. *Synth. Commun.* **2018**, *48*, 1099–1127.
- Akduman, B.; Crawford, E.D. Terazosin, doxazosin, and prazosin: Current clinical experience. *Urology* **2001**, *58*, 49–54.
- Patel, H.M.; Ahmad, I.; Pawara, R.; Shaikh, M.; Surana, S. In silico search of triple mutant T790M/C797S allosteric inhibitors to conquer acquired resistance problem in non-small cell lung cancer (NSCLC): A combined approach of structure-based virtual screening and molecular dynamics simulation. *J. Biomol. Struct. Dyn.* **2021**, *39*, 1491–1505.
- Kassem, M.G. Gefitinib AFM Motiur Rahman\*, Hesham M. Korashy. *Profiles Drug Subst. Excip. Relat. Methodol.* **2014**, *239*.
- Cheng, W.; Wang, S.; Yang, Z.; Tian, X.; Hu, Y. Design, synthesis, and biological study of 4-[(2-nitroimidazole-1H-alkyloxy) aniline]-quinazolines as EGFR inhibitors exerting cytotoxicities both under normoxia and hypoxia. *Drug Des. Dev. Ther.* **2019**, *13*, 3079.
- Geyer, C.E.; Forster, J.; Lindquist, D.; Chan, S.; Romieu, C.G.; Pienkowski, T.; Cameron, D. Lapatinib plus capecitabine for HER2-positive advanced breast cancer. *N. Engl. J. Med.* **2006**, *355*, 2733–2743.
- Mari, A.; Antonelli, A.; Cindolo, L.; Fusco, F.; Minervini, A.; De Nunzio, C. Alfuzosin for the medical treatment of benign prostatic hyperplasia and lower urinary tract symptoms: A systematic review of the literature and narrative synthesis. *Ther. Adv. Urol.* **2021**, *13*, 17562872211993283.
- Kikuchi, H.; Horoiwa, S.; Kasahara, R.; Hariguchi, N.; Matsumoto, M.; Oshima, Y. Synthesis of febrifugine derivatives and development of an effective and safe tetrahydroquinazoline-type antimalarial. *Eur. J. Med. Chem.* **2014**, *76*, 10–19.
- Khan, I.; Ibrar, A.; Ahmed, W.; Saeed, A. Synthetic approaches, functionalization and therapeutic potential of quinazoline and quinazolinone skeletons: The advances continue. *Eur. J. Med. Chem.* **2015**, *90*, 124–169.
- Vinoth, S.; Devi, K.S.; Pandikumar, A. A comprehensive review on graphitic carbon nitride based electrochemical and biosensors for environmental and healthcare applications. *TrAC Trends Anal. Chem.* **2021**, *140*, 116274.
- Akhundi, A.; Badiei, A.; Ziarani, G.M.; Habibi-Yangjeh, A.; Munoz-Batista, M.J.; Luque, R. Graphitic carbon nitride-based photocatalysts: Toward efficient organic transformation for value-added chemicals production. *Mol. Catal.* **2020**, *488*, 110902.
- Azhdari, A.; Azizi, N.; Sanaeishoar, H.; Tahanpesar, E. Amidosulfonic acid supported on graphitic carbon nitride: Novel and straightforward catalyst for Paal–Knorr pyrrole reaction under mild conditions. *Mon. Für Chem. Chem. Mon.* **2021**, *152*, 625–634.

15. Fatehi, A.; Ghorbani-Vaghei, R.; Alavinia, S.; Mahmoodi, J. Synthesis of Quinazoline Derivatives Catalyzed by a New Efficient Reusable Nanomagnetic Catalyst Supported with Functionalized Piperidinium Benzene-1,3-Disulfonate Ionic Liquid. *ChemistrySelect* **2020**, *5*, 944–951.
16. Rao, A.D.; Vykuntesarao, B.P.; Bhaskarkumar, T.; Jogdand, N.R.; Kalita, D.; Lilakar, J.K.D.; Raghunadh, A. Sulfonic acid functionalized Wang resin (Wang-OSO<sub>3</sub>H) as polymeric acidic catalyst for the eco-friendly synthesis of 2,3-dihydroquinazolin-4 (1H)-ones. *Tetrahedron Lett.* **2015**, *56*, 4714–4717.
17. Dabiri, M.; Salehi, P.; Baghbanzadeh, M.; Zolfigol, M.A.; Agheb, M.; Heydari, S. Silica sulfuric acid: An efficient reusable heterogeneous catalyst for the synthesis of 2,3-dihydroquinazolin-4 (1H)-ones in water and under solvent-free conditions. *Catal. Commun.* **2008**, *9*, 785–788.
18. Mekala, R.; Madhubabu, M.V.; Dhanunjaya, G.; Regati, S.; Chandrasekhar, K.B.; Sarva, J. Efficient synthesis of 2,3-dihydroquinazolin-4 (1H)-ones catalyzed by titanium silicon oxide nanopowder in aqueous media. *Synth. Commun.* **2017**, *47*, 121–130.
19. Tekale, S.U.; Munde, S.B.; Kauthale, S.S.; Pawar, R.P. An efficient, convenient, and solvent-free synthesis of 2,3-dihydroquinazolin-4 (1H)-ones using montmorillonite-KSF clay as a heterogeneous catalyst. *Org. Prep. Proced. Int.* **2018**, *50*, 314–322.
20. Wang, M.; Zhang, T.T.; Liang, Y.; Gao, J.J. Strontium chloride-catalyzed one-pot synthesis of 2,3-dihydroquinazolin-4 (1H)-ones in protic media. *Chin. Chem. Lett.* **2011**, *22*, 1423–1426.
21. Khan, A.A.; Mitra, K.; Mandal, A.; Baildya, N.; Mondal, M.A. Yttrium nitrate catalyzed synthesis, photophysical study, and TD-DFT calculation of 2,3-dihydroquinazolin-4 (1H)-ones. *Heteroat. Chem.* **2017**, *28*, e21379.
22. Rahmati, M.; Ghafuri, H.; Ghanbari, N.; Tajik, Z. 1,4-Butanesultone functionalized graphitic carbon nitride: Efficient catalysts for the one-pot synthesis of 1,4-dihydropyridine and polyhydroquinoline derivative through hantzsch reaction. *Polycycl. Aromat. Compd.* **2022**, *42*, 3019–3035.